IOPscience iopscience.iop.org

Home Search Collections Journals About Contact us My IOPscience

Transient response of relativistic electron bunches to wave-number selected perturbations near the micro-bunching instability threshold

This content has been downloaded from IOPscience. Please scroll down to see the full text.

2014 New J. Phys. 16 063027

(http://iopscience.iop.org/1367-2630/16/6/063027)

View the table of contents for this issue, or go to the journal homepage for more

Download details:

IP Address: 133.48.171.227
This content was downloaded on 16/06/2014 at 01:45

Please note that terms and conditions apply.

New Journal of Physics
The open access journal at the forefront of physics
Deutsche Physikalische Gesellschaft DPG | IOP Institute of Physics

Transient response of relativistic electron bunches to wave-number selected perturbations near the micro-bunching instability threshold

E Roussel[1], C Evain[1], M Le Parquier[1], C Szwaj[1], S Bielawski[1], M Hosaka[2], N Yamamoto[2], Y Takashima[2], M Shimada[3], M Adachi[4], H Zen[4], S Kimura[4] and M Katoh[4]

[1] Laboratoire de Physique des Lasers, Atomes et Molécules, UMR CNRS 8523, and Centre d'Études et de Recherches Lasers et Applications, Université Lille 1, Sciences et Technologies, F-59655 Villeneuve d'Ascq Cedex, France
[2] Graduate School of Engineering, Nagoya University, Nagoya, 464-8603, Japan
[3] High Energy Accelerator Research Organization, KEK, Tsukuba, 305-0801, Japan
[4] UVSOR Facility, Institute for Molecular Science, National Institutes of Natural Sciences, Okazaki 444-8585, Japan
E-mail: serge.bielawski@univ-lille1.fr

Received 29 December 2013, revised 17 April 2014
Accepted for publication 1 May 2014
Published 13 June 2014

New Journal of Physics **16** (2014) 063027

doi:10.1088/1367-2630/16/6/063027

Abstract

Many spatio-temporal systems can undergo instabilities, leading to the spontaneous formation of spatial structures (patterns). However, a range of cases exist for which the pattern itself is not directly visible because of technical or fundamental reasons. This is the case for the spontaneous formation of millimeter-scale patterns appearing inside relativistic electron bunches of accelerators. We demonstrate in this case how the study of responses to sine external perturbations can be used as a 'probe' to deduce the characteristic wavenumber of the pattern formation process. Experiments are performed in the UVSOR-II electron storage ring when the electron bunch is subjected to so-called microbunching instability, and the sine perturbations are provided by an external laser. The response is constituted of pulses of coherent synchrotron radiation, whose amplitude depends on the perturbation wavenumber. Experimental results on the dynamics are compared to numerical calculations obtained using a Vlasov–Fokker–Planck model.

Content from this work may be used under the terms of the Creative Commons Attribution 3.0 licence.
Any further distribution of this work must maintain attribution to the author(s) and the title of the work, journal citation and DOI.

© 2014 IOP Publishing Ltd and Deutsche Physikalische Gesellschaft

S Online supplementary data available from stacks.iop.org/njp/16/063027/mmedia

Keywords: accelerators, pattern formation, Vlasov, synchrotron radiation, instabilities

In a relativistic electron bunch, interactions between electrons through electric forces (wakefields) can be the cause of so-called microbunching instability [1–9], which is characterized by the spontaneous formation of patterns in the electron bunch phase space [10–12]. The understanding of this dynamics is crucial, as electron storage rings are extremely important sources for users of radiation in the VUV, x-ray, and THz ranges. However, in contrast to more classical pattern-forming systems, as in hydrodynamics, chemistry, biology, optics, etc [13], the study of pattern formation in relativistic electron bunches presents additional difficulties because of the very indirect nature of the possible measurements. This situation is illustrated in figure 1, where we have represented a typical phase space computed numerically using the parameters of the UVSOR-II storage ring. Above a threshold current, a two-dimensional pattern is spontaneously formed (figures 1(b), (c)) and its evolution in time t is usually extremely rich and complex, as the structures continuously rotate in phase space, and appear in a bursting manner. In contrast, the experimental data contain much less information because they usually consist of the recording of the coherent submillimeter/millimeter radiation (CSR) emitted by the structures using bolometers (figures 1(d), (e)), or diode detectors. In other words, the detected signal $D(t)$ can be viewed mathematically as a projection of the two-dimensional pattern $f\left(z, \delta e, t\right)$ onto a scalar variable $D(t)$:

$$f\left(z, \delta e, t\right) \rightarrow D\left(t\right) = \int_{-\infty}^{+\infty} H\left(k\right) \left| \int_{-\infty}^{+\infty} \int_{-\infty}^{+\infty} f\left(z, \delta e, t\right) \exp\left(-ikz\right) dz d\delta e \right|^2 dk$$
$$= \int_{-\infty}^{+\infty} H\left(k\right) FF\left(k, t\right) dk, \quad (1)$$

with $H(k)$ a transfer function, and $FF\left(k, t\right)$ the so-called form factor [14] of the electron bunch at time t. The details of this projection are not important at this stage. However, this already shows that most of the information on the two-dimensional pattern $f\left(z, \delta e, t\right)$ is lost, and that even crucial features such as the wavenumber selected at the instability threshold are difficult to access[5] from the detected signal $D(t)$.

In this article, we present an alternate approach that consists of systematically examining the system's transient response to initial perturbations with selected wavenumbers for various values of the main operating parameter. From common knowledge in nonlinear dynamics, one may indeed expect a huge increase in the system's response when the system is near a phase transition point [13] (the threshold of the microbunching instability here), and the perturbation

[5] In principle, selected wavenumbers may be identified from the spectrum of CSR emission. In this millimeter range spectra are obtained from Fourier Transform spectrometers, which require stable signals. This has been possible in few cases, for particular values of parameters. This has not been possible for instance at UVSOR, where bursting occurs very near threshold.

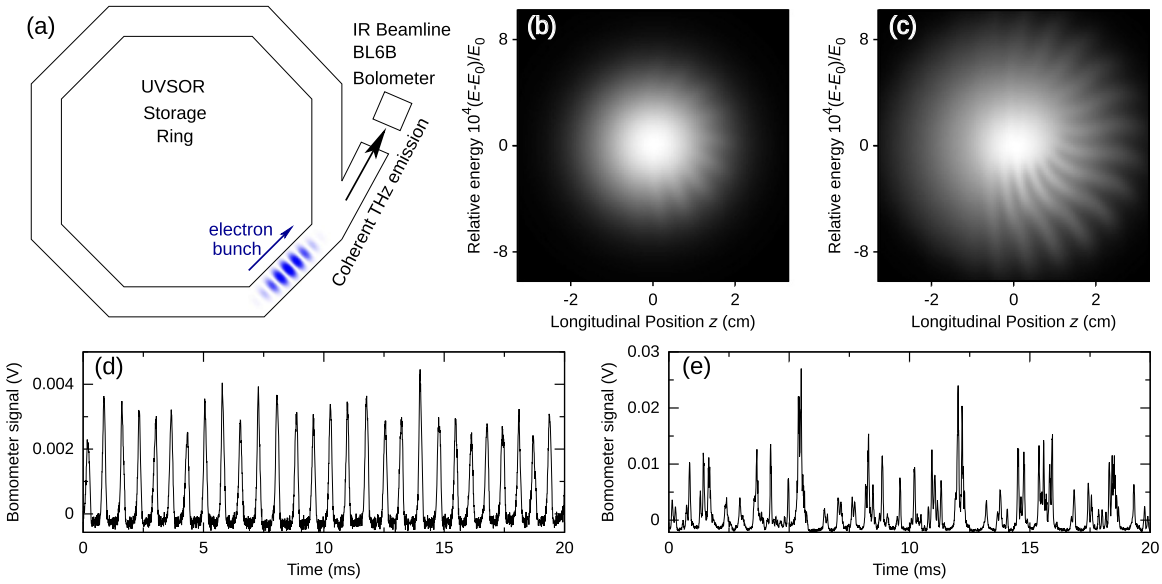

Figure 1. Illustration (theory versus experiment) of the microbunching instability issue in storage rings. (a) A relativistic electron bunch (600 MeV, with the length in the centimeter range for UVSOR-II) experiences round-trips in a vacuum chamber. If the electron bunch charge exceeds a given threshold, a spatiotemporal instability leads to the spontaneous formation of patterns inside the electron bunch density, which is responsible for the emission of strong millimeter and terahertz radiation in the bending magnets. (b), (c) A typical pattern in phase space computed from the classical Fokker–Planck–Vlasov model (the integration of equation (2) for currents of 4.5 mA (b) and 12 mA (c), and the parameters from table (1)). The pattern rotates in phase space with a frequency of the order of 10 kHz, and its evolution is usually irregular. In contrast, the data typically available experimentally (d), (e), contain much less information, as they consist of single bolometer signals versus time. Most of the information on the two-dimensional structure, as its characteristic wavenumber, are thus not accessible. The currents for (d) and (e) are 11.1 mA and 12.9 mA, respectively. Movies of (b) and (c) can be found in the supplementary material, available at stacks.iop.org/njp/16/036027/mmedia.

has a wavenumber close to the characteristic wavenumber of the instability. From a conceptual point of view, this perturbation strategy is close to the experiments performed in the Rayleigh–Bénard experiments [15], although our goal is different here.

Technically, this attempt to use laser perturbations to probe the pattern formation is also motivated by the pioneering work of Byrd, Sannibale *et al* [16]. They demonstrated that a huge response (a burst of intense coherent synchrotron radiation) can be obtained using short laser pulses. Here, instead of using short pulses (and thus a broadband initial perturbation), a key point is of course to shape the laser pulses with a sine profile [17] (at millimeter scale). The sinusoidally shaped laser pulses that are chosen are moreover slightly longer than the electron bunch (several centimeters) (figure 2(a)).

The experiments were conducted in the UVSOR-II storage ring, operating at an energy of $E_0 = 600$ MeV, in single-bunch low-alpha mode [18] (the machine parameters are displayed in table 1). In these conditions, the electron bunch has a duration of 37 ps RMS at low current, a relative energy spread $\sigma_E/E_0 = 3.4 \times 10^{-4}$ RMS, and the threshold for the microbunching

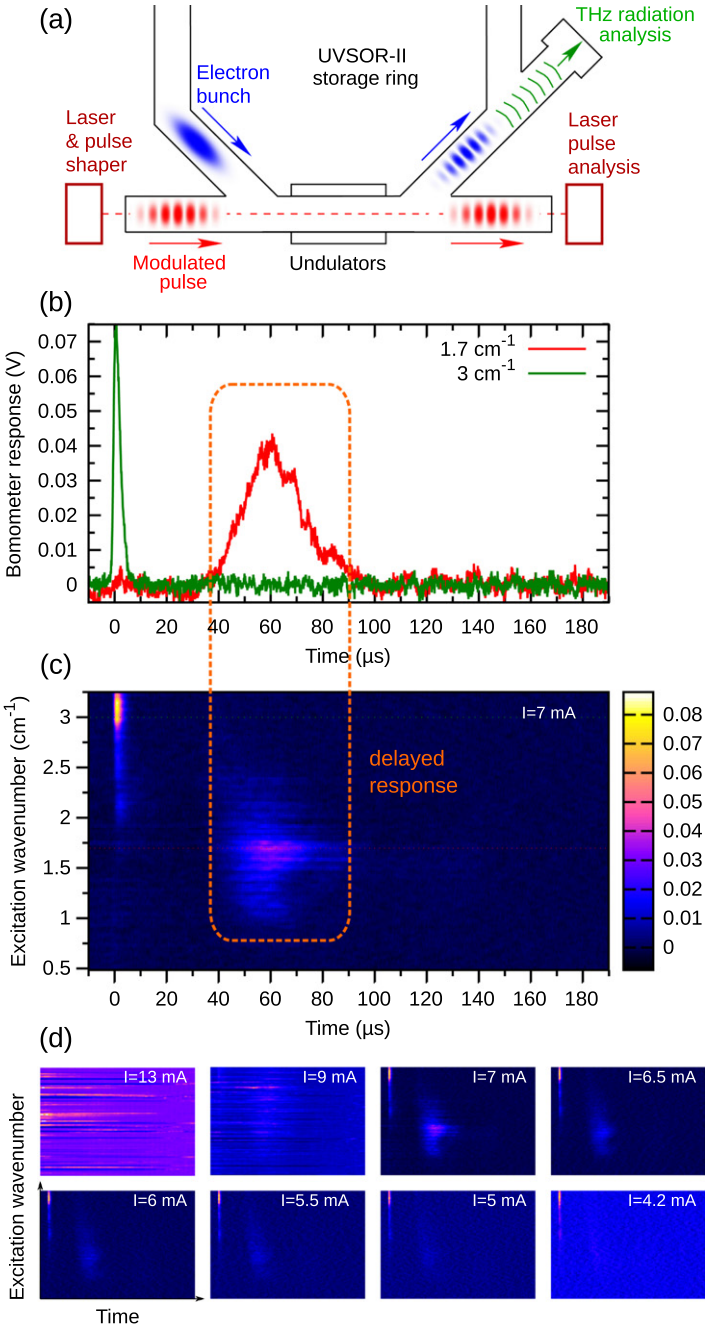

Figure 2. The experimental 'seeding' of patterns using sinusoidally modulated laser perturbations. (a) The setup for the sine perturbations of the electron bunch. (b) Bolometer signal versus time for two modulation wavenumbers: $\bar{\nu}_m = 1.7$ cm^{-1} (strong pattern seeding is visible as a delayed response around $t = 60$ μs) and $\bar{\nu}_m = 3$ cm^{-1} (no noticeable seeding occurs). (c) Bolometer signal versus time and modulation wavenumbers, showing that seeding is effective only for wavenumbers around 1.7 cm^{-1}. The current is $I = 7$ mA. (d) The evolution of figure (c) with the current.

Table 1. The parameters corresponding to the experiment and used in the numerical simulations. Note that the natural bunch length is the value at zero current (the actual length is longer at finite current).

Nominal energy	$E_0 = 600$ MeV
Energy spread	$\sigma_E = 0.204$ MeV RMS
Relative energy spread	$\sigma_\delta = \sigma_E/E_0 = 3.4 \times 10^{-4}$ RMS
Natural bunch length	36.6 ps RMS ($\sigma_z = 10.98$ mm RMS)
Laser pulse duration	300 ps FWHM (38.2 mm RMS)
Revolution period	$T_0 = 177$ ns
Dipole radius of curvature:	$R = 2.2$ m
Vacuum chamber height:	$2\,h = 3.8 \times 10^{-2}$ m
Synchrotron frequency	$f_s = 9.09$ kHz
Synchrotron damping time	$\tau_s = 19$ ms
$\left(2\pi f_s \tau_s\right)^{-1}$	$\epsilon = 0.9215 \times 10^{-3}$

instability is typically of the order of 7 mA (i.e. an electron bunch charge of ≈1.2 nC). The bursts of millimeter radiation are monitored by an InSb bolometer (QMC QFI/2) with a 2 μs response time, placed on the BL6B beamline [19]. The laser pulses interact with the electron bunch in an undulator (figure 2(a), and the optical setup is similar to the one described in [17]). We used an amplified laser (Coherent Mira and Legend) delivering 3 mJ, 300 ps FWHM long chirped pulses at 800 nm, and with a 1 kHz repetition rate. These pulses are sinusoidally modulated using the chirped pulse beating technique [20], which allows the modulation period to be chosen simply by adjusting the delay of a Michelson interferometer. The spectroscopic wavenumber $\bar{\nu}_m$ of the perturbation can be typically chosen from the sub-ps range to tens of picoseconds.

The data are recorded as follows. For each chosen sine perturbation wavenumber $\bar{\nu}_m$, we record the transient bolometer temporal trace (which roughly corresponds to the induced pattern amplitude versus time). Furthermore, the responses versus $\bar{\nu}_m$ are systematically recorded versus current I because the effect is expected just below the instability threshold. The data acquisition is automated, using a Lecroy oscilloscope (WR104MXI) in sequence mode, and automatic scanning of the Michelson interferometer. At each current value, we record the responses to 200 values of $\bar{\nu}_m$ from 0.48 to 4.18 cm^{-1} (this takes 8 s). The electron beam current is decreased at a slower rate, using the natural decay of the electron bunch charge, or additional losses when needed.

Schematically, three current zones are observed. At high current (figure 2(d)), the laser has no clear effect, and we simply observe the usual strong bursts of millimeter CSR radiation that already occur spontaneously without the laser (and for which a pattern like the ones in figure 1(b), (c) is expected theoretically). The expected 'pattern seeding' effect is observed for currents that are near the microbunching instability threshold ($I \approx 7$ mA). The signature consists of the delayed pulse [figure 2(b), red curve] at a time of ≈60 μs. The pattern seeding effect then decreases when the current is further decreased to very low values ($I \approx 4-5$ mA and below), where the quasi-instantaneous response to the laser perturbation eventually remains

(this peak near $t = 0$ does not involve the nonlinear dynamics of the system and was studied in [14, 17, 21]).

Furthermore, systematic analysis of this bolometer signal versus modulation wavenumber $\bar{\nu}_m$ reveals that the seeding is effective only in a precise domain of $\bar{\nu}_m$, in the 1.5-2 cm^{-1}range. This effect is clearly visible in figure 2(b), where the green and red curves represent the responses to wavenumber outside and inside the adequate wavenumber range for seeding. This resonance effect appears as a characteristic feature in the colorscale representation of bolometer signals versus $\bar{\nu}_m$ [figure 2(c)], and this feature appears essentially near the instability threshold [figure 2(d)].

We have verified that this peak at $t \approx 60\ \mu$s is unique, using scans of $\bar{\nu}_m$ up to 32 cm^{-1}. Moreover, the relative sizes of the delayed and quasi-immediate responses depend on current, showing that the delayed peak is affected by the effect of wakefields. This will be a main comparison point with theoretical predictions.

A classical framework for theoretical studies is the one-dimensional Vlasov–Fokker–Planck approach. The temporal evolution of the electron density $f\left(q, p, \theta\right)$ reads [11]:

$$\frac{\partial f}{\partial \theta} - p\frac{\partial f}{\partial q} + \left(q - I_c E_{wf}\right)\frac{\partial f}{\partial p} = 2\epsilon\frac{\partial}{\partial p}\left(pf + \frac{\partial f}{\partial p}\right). \tag{2}$$

In this equation, θ is a continuous and dimensionless variable associated with the number of turns in the storage ring: $\theta = 2\pi f_s t$, where t is the time (in seconds) and f_s is the synchrotron frequency (in the tens of kilohertz range here). The longitudinal position q and relative momentum p are the deviation from the so-called synchronous electron (with position z_0 and energy E_0). q and p are expressed in units of the equilibrium bunch length σ_z and energy spread σ_δ at zero current: $q = \left(z - z_0\right)/\sigma_z$, and $p = \left(E - E_0\right)/\sigma_E$. $\epsilon = 1/\left(2\pi f_s \tau_s\right)$, where τ_s is the synchrotron damping time. In usual cases, $\epsilon \ll 1$, meaning that synchrotron oscillations are weakly damped. $I_c = I\frac{e2\pi R}{2\pi f_s \sigma_E T_0}$, with R the dipole radius of curvature, T_0 the revolution period, and I the average beam current (in Amperes). All parameters are in MKS units and $f\left(q, p\right)$ is normalized so that $\int_{-\infty}^{+\infty}\int_{-\infty}^{+\infty} f\left(q, p\right) dqdp = 1$.

E_{wf} characterizes the interaction between electrons, and is the term responsible for the microbunching instability. It represents the average longitudinal electric field created by the whole bunch, per Ampere of currentwakefield created by one electron $E_{wf}^{1e}\left(q\right)$, and the electron bunch charge density [22].

The precise expression of E_{wf}^{1e} is a main ingredient of the modeling, and depends on the electron bunch path and detailed boundary conditions in the accelerator (e.g. the vacuum chamber). For the present test, we use the wakefield produced by an electron on a curved trajectory, between two parallel plates of height $2\,h$, which is one of the simplest models reproducing the experimentally observed dynamics in storage rings [22]. In MKS units, the wakefield $E_{wf}\left(q\right)$ can be expressed as [23]:

$$E_{wf}(q) = \frac{4}{3} \times \frac{\gamma^4 T_0}{4\pi\epsilon_0 R^2} \int_{-\infty}^{+\infty} d\zeta \rho(q-\zeta) w\left(\frac{3\gamma^3}{2R}\sigma_z \zeta\right) - \frac{T_0}{8\pi\epsilon_0 h^2} \int_{-\infty}^{+\infty} d\zeta \rho(q-\zeta) G_2\left(\frac{\sigma_z}{2R(h/R)^{3/2}}\zeta\right), \quad (3)$$

where the functions w and G_2 are given by equations (3.12,5.22b) of [22], and the other parameters are given in table 1. The convolution is computed in Fourier space using an approach similar to the one proposed by Qiang [24] (see [23]). Calculation of the perturbation induced by the laser is detailed in the supplementary data, available at stacks.iop.org/njp/16/063027/mmedia, and

$$\rho(q) = \int_{-\infty}^{+\infty} dp f(q, p) \quad (4)$$

The integration of equation (2) is performed using the semi-Lagrangian approach. The scheme of [25, 26] is implemented using a parallel MPI strategy. The longitudinal q coordinate is divided into slices of equal size, each being associated with a computer core. The computations were performed using a mesh of 400×400 points, with a physical size (in q and p) of 20×20 centered on $(q = 0, p = 0)$, and a time step $h = 2\pi/2000$. The laser perturbation is always applied after the transients have been damped out (typically 1000 synchrotron periods in situations far from the threshold). Sixteen CPU cores are typically used. For comparison with the experiments, the equivalent of the bolometer signal $B(\theta)$ is computed from the electron bunch density distribution $\rho(q)$. The CSR emitted over a $1 - 9.1$ cm^{-1} bandwidth is calculated: $B(\theta) = \int_{k_1}^{k_2} Z_R(k) |\tilde{\rho}(k)|^2 dk$, with Z_R the real part of the CSR impedance [27], $k_1 = 6.9$ and $k_2 = 63$, and $\tilde{\rho}(k)$ the Fourier transform of $\rho(q)$. The bolometer signal $B(\theta)$ is finally processed by a first-order filter, with 2μs response time. We systematically integrated equation (2) for various values of the modulation wavenumber beam current. In addition, since we are interested in the effect of the wakefield on the electron bunch dynamics, we also integrated, in each case, the corresponding equation 'without wakefield' (i.e. taking $I = 0$). This will serve as a reference case, to which departures will be attributed to wakefield effects.

The dynamical behavior is similar to the experimental one, and the simulated bolometer response is composed of two successive peaks (figure 3(e)). As in the experiment, the delayed response around 55-60 μs is strongly enhanced when the modulation wavenumber is around 1.5 cm^{-1} (red curve), and is extremely weak otherwise (green curve). Moreover, we can verify that the delayed peak size is dependent on the collective effects (wakefield), by comparing the data to the reference results 'without wakefield' (i.e. $I = 0$ and all other parameters unchanged, black curve). The phase space evolution is represented in figures 3(a)–(d). Analyses versus the excitation wavenumber (figure 3(f)) confirms that the maximum delayed response occurs at $\bar{\nu}_m \approx 1.5$ cm^{-1}.

Further study of wavenumber selection can be performed by plotting the height of the delayed peak versus modulation wavenumber. As expected (figure 4(a)), a good agreement between theory and experiment is found. Furthermore, it is instructive to compare these

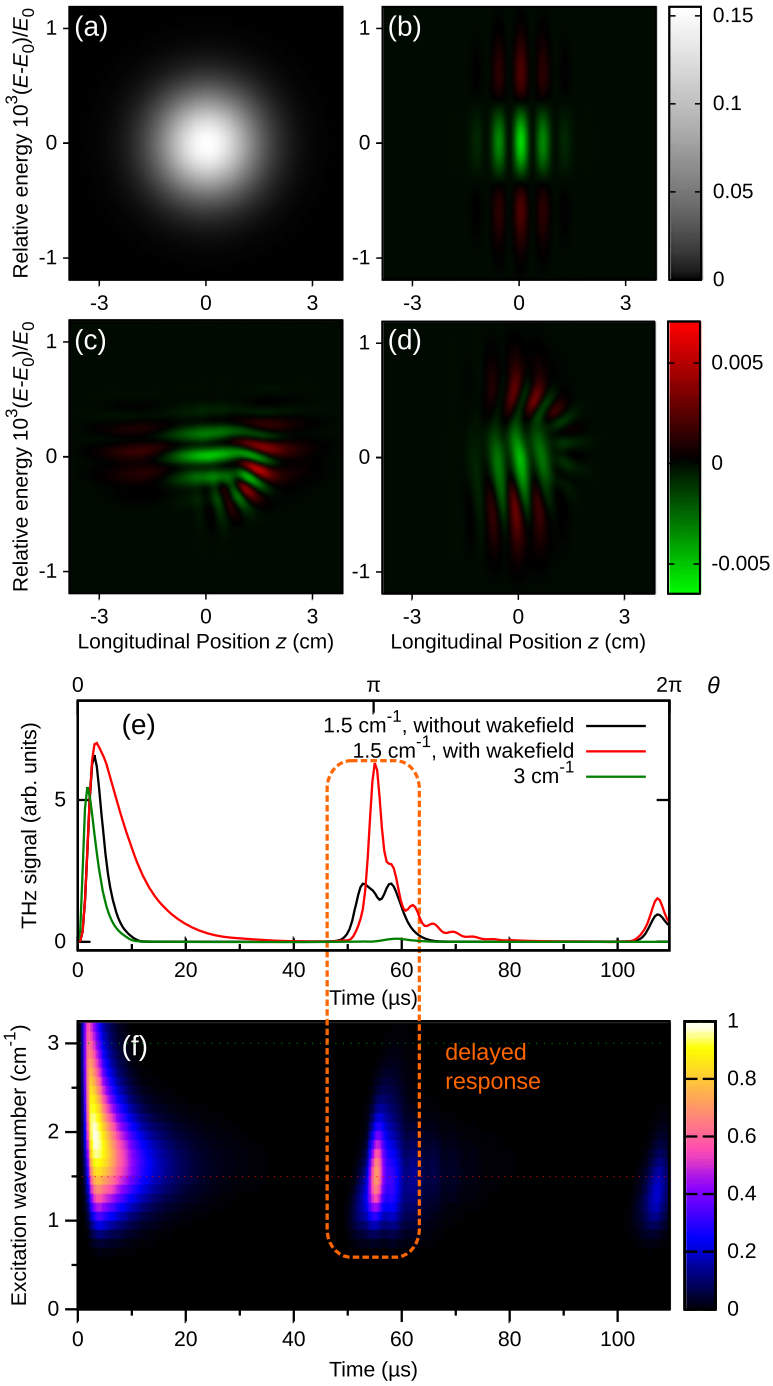

Figure 3. Numerical calculations of the response to a modulated laser perturbation (with $\bar{\nu}_m$=1.5 cm^{-1} and I = 3.5 mA). (a) The phase space just before laser modulation, (b)–(d) the phase space at different times after the laser perturbation: $\theta = 0$, $\pi/2$, π, respectively (for clarity, the initial phase space distribution (a) has been subtracted), (e) the deduced bolometer signals, and (f) the bolometer signal versus excitation wavenumber. Note that $\theta = 2\pi$ corresponds to one synchrotron period (110 μs).

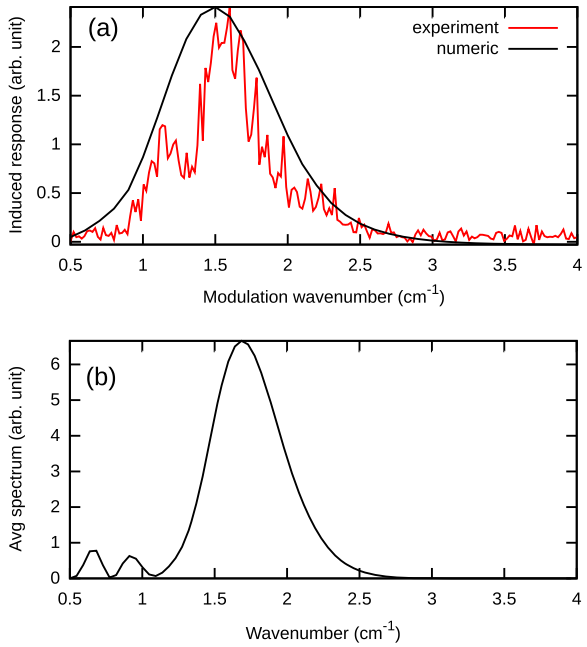

Figure 4. The characteristic wavenumbers of the instability. (a) Laser seeding strategy: height of the delayed peak versus $\bar{\nu}_m$ (red: experiment, black: numerical simulation). (b) CSR emission spectrum above threshold without laser perturbation (simulation, I = 4.5 mA).

curves with the CSR spectrum of the 'free-running system' (i.e. without laser seeding) above the instability threshold. The emitted spectrum (figure 4(b)) is found to coincide with the tuning curve of figure 4(a), and this agreement was found for all currents in this zone. This shows that the seeding strategy is a promising technique for examining the characteristic wavenumbers of the instability.

As this technique provides new possibilities for testing theories, we also tried to find possible differences between the theoretical and experimental findings. One difference is the ratio between the delayed response and the immediate one (the ratio is larger experimentally, as can be seen in the red curves of figures 2(b) and 3(e)). Further refinement of the theory is beyond the scope of this paper. However, we believe that this type of experiment may also point out differences between the observations and existing models in other storage rings, and help progress in refining existing theories (e.g. wakefields).

In conclusion, the manipulation of a relativistic electron bunch using specially shaped laser pulses allows us to obtain dynamical information on the spatio-temporal instability occurring in relativistic electron bunches circulating in a storage ring. This information includes the characteristic wavenumber and the shape of the transients occurring after perturbation. The present test at UVSOR-II reveals a satisfying agreement with the Vlasov–Fokker–Planck equation with a parallel-plates wakefield. Tests in other accelerators are possible *a priori* when a laser perturbation is achievable, in particular in storage rings equipped with a laser slicing setup.

Acknowledgments

We would like to thank LeCroy for providing the oscilloscope in the first experiments. This work was supported by the Joint Studies Program of the IMS, the JSPS fellowship program for research in Japan (S-09171), the PICS project from CNRS, the Grant-in-aid for scientific researches (B20360041) of JSPS, and the ANR (Blanc 2010-042301), and used HPC resources from GENCI TGCC/IDRIS (2013-x2013057057). CERLA is supported by the French Ministère chargé de la Recherche, the Région Nord-Pas de Calais, and the FEDER.

References

[1] Byrd J M, Leemans W P, Loftsdottir A, Marcelis B, Martin M C, McKinney W R, Sannibale F, Scarvie T and Steier C 2002 Observation of broadband self-amplified spontaneous coherent terahertz synchrotron radiation in a storage ring *Phys. Rev. Lett.* **89** 224801

[2] Abo-Bakr M, Feikes J, Holldack K, Wüstefeld G and Hübers H-W 2002 Steady-state far-infrared coherent synchrotron radiation detected at bessy ii *Phys. Rev. Lett.* **88** 254801

[3] Sannibale F, Byrd J M, Loftsdóttir Á, Venturini M, Abo-Bakr M, Feikes J, Holldack K, Kuske P, Wüstefeld G, Hübers H-W and Warnock R 2004 A model describing stable coherent synchrotron radiation in storage rings *Phys. Rev. Lett.* **93** 094801

[4] Feikes J, von Hartrott M, Ries M, Schmid P, Wüstefeld G, Hoehl A, Klein R, Müller R and Ulm G 2011 Metrology light source: the first electron storage ring optimized for generating coherent thz radiation *Phys. Rev. ST Accel. Beams* **14** 030705

[5] Hashimoto S, Shoji Y, Ando A and Takahashi T 2005 Observation of coherent synchrotron radiation at newsubaru *Proc. 2005 Particle Accelerator Conf. (Knoxville, TN)* pp 4188–90

[6] Karantzoulis E, Penco G, Perucchi A and Lupi S 2010 Characterization of coherent THz radiation bursting regime at elettra *Infrared Physics and Technology* **53** 300

[7] Shields W, Bartolini R, Boorman G, Karataev P, Lyapin A, Puntree J and Rehm G 2012 Microbunch instability observations from a THz detector at diamond light source *J. Phys.: Conf. Ser.* **357** 012037

[8] Mochihashi A, Hosaka M, Katoh M, Shimada M and Kimura S 2006 Observation of THz synchrotron radiation burst in UVSOR-II electron storage ring *Proc. 2006 European Particle Accelerator Conf. (Edinburgh, Scotland)* p 3380

[9] Evain C *et al* 2012 Spatio-temporal dynamics of relativistic electron bunches during the micro-bunching instability in storage rings *Europhys. Lett.* **98** 40006

[10] Stupakov G and Heifets S 2002 Beam instability and microbunching due to coherent synchrotron radiation *Phys. Rev. ST Accel. Beams* **5** 054402

[11] Venturini M, Warnock R, Ruth R and Ellison J A 2005 Coherent synchrotron radiation and bunch stability in a compact storage ring *Phys. Rev. ST Accel. Beams* **8** 014202

[12] Warnock R L 2006 Study of bunch instabilities by the nonlinear Vlasov–Fokker–Planck equation *Nucl. Instrum. Meth. Phys. Res., Sect.* A **561** 186–94

[13] Cross M C and Hohenberg P C 1993 Pattern formation outside of equilibrium *Rev. Mod. Phys.* **65** 851–1112

[14] Hosaka M *et al* 2013 Saturation of the laser-induced narrowband coherent synchrotron radiation process: experimental observation at a storage ring *Phys. Rev. ST Accel. Beams* **16** 020701

[15] Perkins A C, Grigoriev R O and Schatz M F 2011 Modal spectra extracted from nonequilibrium fluid patterns in laboratory experiments on rayleigh-bénard convection *Phys. Rev. Lett.* **107** 064501

[16] Byrd J M, Hao Z, Martin M C, Robin D S, Sannibale F, Schoenlein R W, Zholents A A and Zolotorev M S 2006 Laser seeding of the storage-ring microbunching instability for high-power coherent terahertz radiation *Phys. Rev. Lett.* **97** 074802

[17] Evain C *et al* 2010 Laser-induced narrowband coherent synchrotron radiation: efficiency versus frequency and laser power *Phys. Rev. ST Accel. Beams* **13** 090703

[18] Shimada M, Adachi M, Katoh M, Kimura S, Hosaka M, Takashima Y, Yamamoto N, Takahashi T and Tanikawa T 2009 Transverse-longitudinal coupling effect in laser bunch slicing *Phys. Rev. Lett.* **103** 144802

[19] Kimura S, Nakamura E, Nishi T, Sakurai Y, Hayashi K, Yamazaki J and Katoh M 2006 Infrared and terahertz spectromicroscopy beam line BL6B(IR) at UVSOR-II *Infrared Physics and Technology* **49** 147– 151

[20] Weling A S and Auston D H 1996 Novel sources and detectors for coherent tunable narrow-band terahertz radiation in free space *J. Opt. Soc. Am.* B **13** 2783–91

[21] Bielawski S *et al* 2008 Tunable narrowband terahertz emission from mastered laser-electron beam interaction *Nature Physics* **4** 390–3

[22] Murphy J B, Krinsky S and Gluckstern R L 1996 Longitudinal wake field for an electron moving on a circular orbit *Part. Accel.* **57** 56

[23] Roussel E, Evain C, Szwaj C and Bielawski S 2014 Microbunching instability in storage rings: link between phase-space structure and terahertz coherent synchrotron radiation radio-frequency spectra *Phys. Rev ST Accel. Beams* **17** 010701

[24] Qiang J 2010 A high-order fast method for computing convolution integral with smooth kernel *Computer Physics Communications* **181** 313–6

[25] Warnock R and Ellison J A 2000 The physics of high brightness beams *Proc. II ICFA advanced accelerator workshop* (Singapore: World Scientific) p 322

[26] Warnock R and Ellison J A 2000 A general method for propagation of the phase space distribution, with application to the sawtooth instability *Proc. 2nd ICFA Advanced Workshop on The Physics of High Brightness Beams (University of California, LA, 1999)* SLAC PUB **8404** 322–48

[27] Chao A W and Tigner M (ed) 1999 *Accelerator Physics and Engineering* (Singapore: World Scientific)